Special Issue Nano-structure Controls of Functional Powders

特集

Research Report

Evolution of the Morphology of Zinc Oxide/Silica Particles Made by Spray Combustion

Takao Tani, Kazumasa Takatori, Sotiris E. Pratsinis

噴霧火炎合成した酸化亜鉛／シリカ粒子の形態

谷孝夫，鷹取一雅，ソティリス・プラティニス

Abstract

Pure and mixed ZnO-SiO_2 particles were prepared by flame spray pyrolysis (FSP) of zinc acetate (ZA) and either hexamethyldisiloxane (HMDSO) or SiO_2-sol dispersed in either methanol or a water-in-oil emulsion. The product particles were characterized by nitrogen adsorption, infrared absorption and X-ray diffraction. The evolution of solid or hollow particle formation along the flame axis was elucidated by observing particles collected in the spray flame by thermophoretic sampling. The effects of using different silicon precursors and solvents on product particle characteristics were evaluated. The characteristics of the product particles can be controlled by the Si precursor and solvent.

Keywords Flame spray pyrolysis, Nanoparticles, Zinc oxide, Silica, Particle morphology

要　旨

ZnO，SiO_2およびZnO/SiO_2粒子を噴霧火炎合成した。酢酸亜鉛をZn源，ヘキサメチルシロキサンまたはSiO_2ゾルをSi源とし，メタノールまたは油中水型エマルションを溶媒とした。合成粒子の特性を窒素吸着，赤外吸収，X線回折によって評価し，粒子特性に及ぼすシリコン源および溶媒の影響を把握した。粒子を噴霧火炎中でサンプリングし透過型電子顕微鏡観察することにより，火炎中での粒子生成過程を明らかにした。粒子特性がSi源および溶媒によって制御されることを示した。

キーワード　噴霧火炎合成，ナノ粒子，酸化亜鉛，シリカ，粒子形態

特集

1. Introduction

Flame synthesis is an established process to produce oxide nanoparticles. Flame reactors are advantageous as they do not involve many steps of wet chemistry, have no moving parts and can produce high purity particles (e. g. manufacture of lightguide preforms) that can be readily separated from their carrier gases.[1] Flame spray pyrolysis (FSP),[2-5] in particular, is a promising technique because a variety of precursors can be used compared with conventional flame aerosol synthesis, where gas-phase precursors (e. g. metal chlorides and metal organics) are needed.[6] In addition, the high flame temperature of FSP can form highly crystalline, and thus thermally stable, particles in one-step compared with liquid-phase-made particles .[7] Therefore, FSP is advantageous, especially for preparation of multi-component optical or catalytic materials.

Various spray aerosol processes have been investigated in preparation of ZnO/SiO_2 mixed oxide particles due to their unique optical properties. Mikrajuddin et al.[8] used a combination of sol-gel synthesis and spray drying to produce ZnO/SiO_2 composite particles where ZnO crystals (~3 nm in size) were dispersed in amorphous SiO_2 to stabilize the photoluminescence of the ZnO nano-crystals. Tani et al.[9] prepared nano-composite ZnO/SiO_2 particles of less than 10 nm in diameter with controlled ZnO crystal size (1.2 to 3.9 nm) by varying the precursor composition during FSP. These particles exhibited a blue shift of UV-light and performed as quantum dots.[10] On the other hand, Kang and Park[11] investigated synthesis of α-willemite (Zn_2SiO_4), a typical host material for green phosphor in plasma display panels,[12] by spray pyrolysis (SP) and reported that SP at low temperatures (i. e. <1000 ^oC) formed a mixture of ZnO and β-willemite, which was transformed by calcination at 1200 ^oC to α-willemite. Tani et al.[13] showed that calcination of FSP-made $2ZnO/SiO_2$ nano-composite particles resulted in β-willemite with crystal growth of ZnO after 2 hours at 800 ^oC while it formed α-willemite particles of ~50 nm in diameter after 2 hours at 900 ^oC. Lenggoro et al.[14] obtained pure α-willemite directly by SP at high temperatures (e. g. 1300 ^oC) and a long residence time (~4 s).

The morphology and/or crystallinity of FSP-made particles can be controlled by the precursor solution composition. Mädler and Pratsinis[15] showed that bismuth nitrate in methanol and bismuth acetate in acetic acid resulted in large (e. g. 1 μm) hollow Bi_2O_3 particles and nanometer-sized solid particles, respectively. Combustion of water-in-oil (w/o) emulsions containing metal precursors can also be used to make solid or hollow ceramic particles, by the so-called emulsion combustion method (ECM).[16-18] Tani et al.[19] showed that ECM can produce a variety of hollow or solid metal oxide particles (e. g. Al_2O_3, TiO_2, ZrO_2 etc.) of variable shell thickness.

Although all previous studies have shown how various process parameters can control the characteristics of FSP- or ECM-made ZnO/SiO_2, they have treated the flame as a "black box". The goal of the present study is to understand particle formation by FSP and ECM from various precursors using the same reactor to unravel the effect of precursors, solvent states and processes on the formation of the particles. Furthermore, thermophoretic sampling[20, 21] of the particles in the flame was applied to elucidate the evolution of particle morphology along the flame axis. Finally, the particles produced were characterized by nitrogen adsorption, energy dispersive X-ray spectroscopy, infrared spectroscopy, X-ray diffraction and microscopy.

2. Experimental

Zinc acetate (ZA) and either a SiO_2-sol or hexamethyldisiloxane (HMDSO) were used as Zn and Si sources, respectively. These precursors were dissolved or dispersed in methanol, resulting in solutions (or stable suspensions) of 0.5 mol/L in total metal ion concentration for all FSP experiments. A w/o emulsion was prepared from deionized water, kerosene and a surfactant (hexa (2-hydroxy-1, 3-propylene-glycol) diricinoleate) for ECM experiments, where the ZA and/or the SiO_2-sol were dissolved (or dispersed) in water and the HMDSO was mixed with kerosene. Hydrogen peroxide was added (5 vol%) into the aqueous phase

to stabilize the emulsion spray flame. The total metal ion concentration in the emulsions was adjusted to 0.5 mol/L as for the FSP solutions. The aqueous phase, the oil phase and the surfactant were mixed at volume ratios of 65, 33.5 and 1.5, respectively, and stirred at 10,000 rpm for 10 min, forming w/o emulsions with aqueous microspheres of 1-2 μm in diameter dispersed in the oil phase.

Powder synthesis was carried out using a spray flame reactor (**Fig. 1**). The detailed configurations of the reactor and experimental conditions are reported elsewhere.[22] For the methanol (FSP) and w/o emulsion (ECM) spray flames, the adiabatic temperatures[23, 24] were 3250 and 2280 °C and the flame heights were about 8 and 10 cm, respectively, without the metal precursors.

The particle morphology was observed by transmission electron microscopy (TEM). The compositional analysis was carried out by energy dispersive X-ray spectroscopy (EDS). The crystallinity was evaluated by X-ray diffraction (XRD) at 2θ (Cu-Kα) = 20-70° and scan speed = 2°/min. The ZnO crystalline size (d_{XRD}) was calculated using Scherrer's equation[25] from the full width at half maximum (FWHM) of the (100) peak after correcting for peak broadening derived from the equipment by measuring the FWHM of several micrometer-sized ZnO particles. The specific surface area (SSA) was determined by nitrogen adsorption after degassing the powder at 150 °C for 20 min in nitrogen. The BET-equivalent average primary particle diameter (d_{BET}) was obtained from the measured SSA and solid density (ρ) using $d_{BET} = 6 / (SSA \times \rho)$ assuming solid spherical particles. For this calculation, literature values of ρ = 5.6 Mg/m^3(ZnO) and 2.2 Mg/m^3 (SiO_2)[26] were used whereas a density estimated based on a 2/3 ZnO + 1/3 SiO_2 mixture (4.5 Mg/m^3) was used for $2ZnO/SiO_2$ because the fractions of zinc silicates were unknown and the theoretical densities of β-willemite (4.3 Mg/m^3, #14-0653) and $Zn_{1.7}SiO_4$ (3.9 Mg/m^3, #24-1466) were similar to that of a 2/3 ZnO + 1/3 SiO_2 mixture. Infrared (IR) absorption spectra of the powder were obtained by IR spectroscopy. For thermophoretic sampling, a copper mesh (3 mm in diameter) covered with carbon film was set on the sampling head, which was driven by compressed air at an average velocity of 1 m/s and held in the center of the flame for 50 ms to collect particles. The obtained particles were also observed by TEM. All powders are labeled by product (ZnO: Z, SiO_2: S or $2ZnO/SiO_2$: ZS); process (FSP: F or ECM: E); and silicon precursor (HMDSO: H or SiO_2-sol: S), so that $2ZnO/SiO_2$ made by FSP using HMDSO is labeled as ZS-F-H, for example.

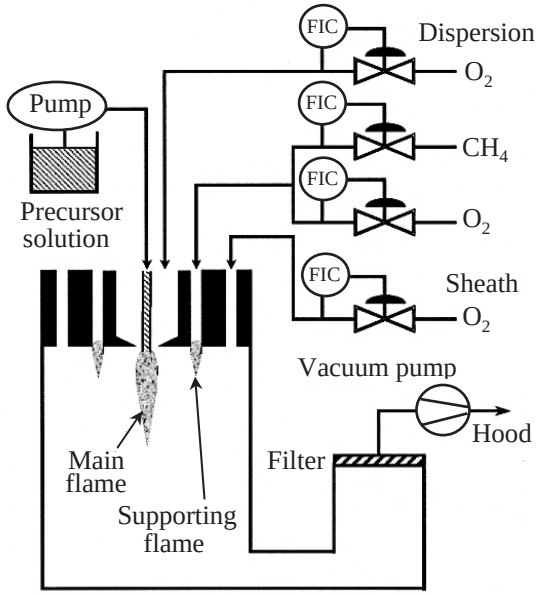

Fig. 1 A schematic of the flame spray reactor used for particle synthesis.

3. Results and discussion

3. 1 Morphology

Figure 2 shows TEM images of the FSP- or ECM-made ZnO and SiO_2 particles. Polyhedral aggregates of nanoparticles, observed typically with flame-made particles,[1] are obtained for the ZnO (Z-F and Z-E) and HMDSO-derived SiO_2 powders (S-F-H and S-E-H) regardless of the process (FSP or ECM: Fig. 2(a)-(d)). This result indicates that these oxides are formed by a gas phase reaction. Apparently, the ZA and HMDSO precursors rapidly evaporate from the droplets and form nanoparticles by condensation and sintering. Submicrometer-sized spherical particles are obtained for the sol-derived SiO_2 powders (S-F-S and S-E-S), again regardless of the process (Fig. 2(e), (f)). This result suggests that the Si species (e. g. atoms, ions or oxide clusters) does not evaporate from the SiO_2-sol particles in the

flame, instead forming aggregates by evaporation of the solvent in the droplets. Judging from the contrast in the TEM image (Fig. 2(e)), the S-F-S powder seems to consist of hollow and solid particles, the diameters of which are far smaller than the dispersed droplet size (e. g. 15 μm in Sauter Mean Diameter), suggesting fragmentation of the droplets in the spray flame. The inhomogeneous particle morphology may result from a size distribution and/or various thermal histories of the fragments in the flame. The S-E-S particles are primarily spherical and hollow with several cavities in the particles, suggesting that they may be aggregates of hollow particles as with ECM-made hollow Al_2O_3 and Y_2O_3 particles.[19] The particle diameters are similar to those of S-F-S. The porous structure is probably formed by fragmentation of the droplets followed by hollow particle formation from aqueous microspheres in the fragments.

Figure 3 shows TEM images of the FSP- or ECM-made $2ZnO/SiO_2$ particles. The powders prepared using HMDSO as Si precursor are comprised of nanoparticles, although few large particles (around 100 nm) co-exist (Fig. 3(a),(b)). The nanoparticles are formed by complete evaporation of the Zn- and Si- precursors regardless of the process (FSP or ECM) as seen with the synthesis of the individual pure oxides (Fig. 2(a)-(d)). Intimate mixing of Zn with Si species can suppress ZnO particle growth, resulting in smaller primary particle sizes of ZS-F-H and ZS-E-H than those of Z-F and Z-E, respectively, as with Tani et al.[8] Zinc oxide/silica powders made from the SiO_2-sol as Si precursor (Fig. 3(c), (d)) are a mixture of nanoparticles and large particles (e. g. 100-300 nm) regardless of the combustion process. No hollow particles are seen in the ZS-F-S and ZS-E-S powders, in contrast with the sol-derived SiO_2 powders (Fig. 2(e), (f)).

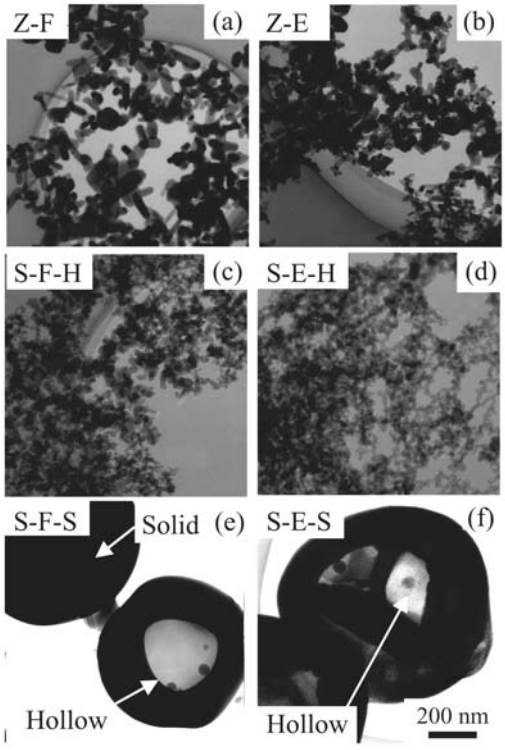

Fig. 2 Morphology of the FSP- or ECM-made ZnO (a, b) and SiO_2 (c, d, e, f) particles. The first sample letter indicates product (ZnO: Z or SiO_2: S) - the second one, the process (FSP: F or ECM: E) - and the third one (for SiO_2), the silicon precursor (HMDSO: H or SiO_2-sol: S). ZnO (a, b) and HMDSO-derived SiO_2 (c, d) resulted in aggregates of nanoparticles indicative of a gas-phase route for particle formation by precursor evaporation, oxidation, coagulation and sintering.

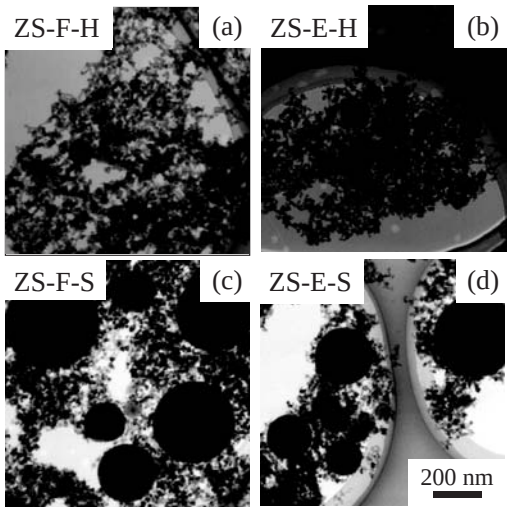

Fig. 3 Morphology of the FSP- or ECM-made $2ZnO/SiO_2$ particles using HMDSO (a, b) and SiO_2-sol (c, d) as Si-precursor. Only nanoparticles were seen for HMDSO-derived $2ZnO/SiO_2$ (a, b) whereas SiO_2-sol-derived $2ZnO/SiO_2$ (c, d) was a mixture of nanoparticles and large particles (e. g. 100-300 nm).

Figure 4 shows EDS spectra of (a) ZS-F-H, (b) large particles in ZS-F-S and (c) nanoparticles in ZS-F-S. The Cu-Lα peak originates from the Cu mesh used for observation. For ZS-F-H (Fig. 4(a)), both Zn and Si are seen in the EDS spectrum, which is similar for several analysis points, suggesting ZnO and SiO_2 are homogeneously mixed. Strong Si-Kα and weak Zn-Lα peaks are seen for the large particles in ZS-F-S (Fig. 4(b)), indicating they are mostly SiO_2. The Zn-Lα peak in the spectrum could result from scattering of the beam and/or nucleation of ZnO from the gas phase onto the large particles. In contrast, the nanoparticles in ZS-F-S (Fig. 4(c)) are primarily ZnO although the EDS spectrum also shows a weak Si-Kα peak, which could also be explained by scattering of the beam and/or partial evaporation of the Si species. The EDS spectra of ZS-E-H and ZS-E-S resemble those of ZS-F-H and ZS-F-S, respectively. These results prove that the nanoparticles and large particles are gas-phase-made ZnO and liquid-phase-made SiO_2, respectively, corresponding to the morphology of the Z-F (or Z-E) and S-F-S (or S-E-S) particles and the XRD results where few (or no) zinc silicates are formed (see **Section 3. 2**). The sizes of the nanoparticles for ZS-F-S and ZS-E-S are smaller than those for Z-F and Z-E, respectively, and also, the large SiO_2 particles for ZS-F-S and ZS-E-S are smaller than those of S-F-S and S-E-S, respetively, although they have broad size distributions. These results will be discussed further (**Section 3. 4**).

3. 2 Crystalline phase and specific surface area

Figure 5 shows XRD spectra of the FSP- and ECM-made ZnO and 2ZnO/SiO_2 powders. The Z-F and Z-E powders (Fig. 5(a), (d)) are hexagonal zincite (#36-1451) with d_{XRD} values of 108 and 53 nm, respectively. The flame temperature used for FSP, higher than that for ECM, can enhance the crystal growth, resulting in a larger d_{XRD} for Z-F than for Z-E. The peaks from zincite are broadened, giving smaller d_{XRD} values of 26 and 27 nm for ZS-F-S and ZS-E-S (Fig. 5(b), (e)), respectively. These results agree well with the TEM observations (Fig. 2 and 3). Few (or no) zinc silicate phases (e. g. β-willemite: #14-0653 and $Zn_{1.7}SiO_4$: #24-1466) are detected for both powders. The similar d_{XRD} values of the two powders indicates that the crystallite size in the mixed oxides is determined by the presence of silica rather than by the combustion conditions as shown by Tani et al.[9] and Mädler et al.[7] During FSP or ECM of ZA and SiO_2-sol, complete evaporation of ZA limits reaction of the Zn compounds with the SiO_2-sol particles in the liquid phase, leading to independent nucleation of ZnO and SiO_2 in the gas and liquid phases, respectively,

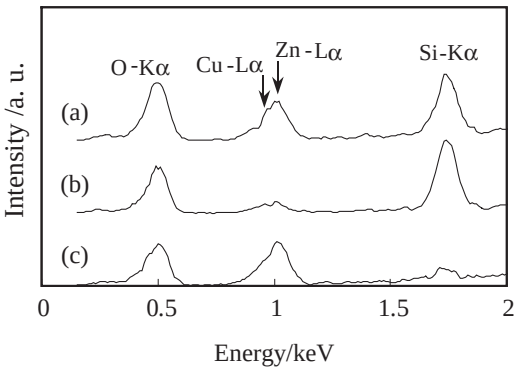

Fig. 4 EDS spectra of (a) HMDSO-derived 2ZnO/SiO_2 (ZS-F-H), (b) large particles in SiO_2-sol-derived 2ZnO/SiO_2 (ZS-F-S) and (c) nanoparticles in ZS-F-S made by FSP. The Si and Zn species were localized in the large particles and nanoparticles, respectively, for ZS-F-S.

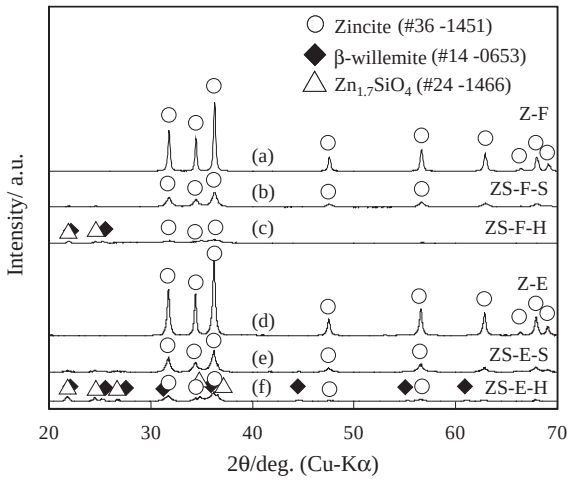

Fig. 5 X-ray diffraction (XRD) patterns of the product powders. Only zincite was detected for ZnO (a, d) and SiO_2-sol-derived 2ZnO/SiO_2 (b, e), whereas very broadened peaks from zinc silicates and zincite were seen for HMDSO-derived 2ZnO/SiO_2 (c, f).

resulting in a mixture of ZnO and SiO_2. On the other hand, FSP or ECM using HMDSO (ZS-F-H and ZS-E-H: Fig. 5(c), (f)) produces a mixture of zincite, β-willemite and $Zn_{1.7}SiO_4$. For ZS-F-H and ZS-E-H, the d_{XRD} values can not be calculated because the diffraction peaks of β-willemite and zincite overlap. These XRD peaks are broadened probably because intimate mixing of the Zn and Si species in the gas phase suppresses each species' particle growth as also described by Tani et al.[9)]

Table 1 summarizes SSA, d_{BET} and d_{XRD} values of the FSP and ECM-made powders. For ZnO, d_{BET} and d_{XRD} of Z-E are smaller than those of Z-F. This result is consistent with the TEM observations (Fig. 2). The difference in d_{XRD} values can be explained by the emulsion spray flame (ECM) having a lower temperature than the methanol spray flame (FSP). Likewise, the d_{BET} of the ECM-made powders is smaller than those of the FSP-made powders produced from the same precursors except for the HMDSO-derived $2ZnO/SiO_2$ powders (ZS-F-H and ZS-E-H). The hollow shell thickness calculated from the d_{BET} ($d_{BET}/3$: ~10 nm)[19)] is far smaller than the shell thickness (e. g. > 100 nm) observed by TEM, suggesting the shell is porous.

Table 1 Specific surface area (SSA), BET-equivalent average primary particle diameter (d_{BET}) and ZnO crystalline size by XRD (d_{XRD}). The sample ID shows product (S: SiO_2, ZS: $2ZnO/SiO_2$ or Z: ZnO), process (F: FSP and E: ECM) and Si precursor (S: the SiO_2-sol or H: hexamethyldisiloxane). The d_{XRD} of ZS-E-S and ZS-F-H could not be calculated (n. c.).

Sample ID	SSA /m^2 g^{-1}	d_{BET} /nm	d_{XRD} /nm
Z-F	23	47	127
ZS-F-H	71	19	n. c.
ZS-F-S	32	41	26
S-F-H	227	12	No data
S-F-S	81	34	No data
Z-E	31	34	53
ZS-E-H	56	24	n. c.
ZS-E-S	39	34	27
S-E-H	338	8	No data
S-E-S	115	24	No data

Judging from the XRD peak heights of the zinc silicates (Fig. 5(c), (f)), ECM seems to enhance the formation of zinc silicates compared to FSP. As it has been reported that $BaTiO_3$ rather than a mixture of BaO (or $BaCO_3$) and TiO_2 is made by ECM,[18)] the longer flame length (particle residence time) and lower temperatures of the emulsion spray flame (ECM) as compared to the methanol spray flame (FSP) can favor the reaction of ZnO with SiO_2.

3. 3 IR spectra

Figure 6 shows IR spectra of the powders. Two absorption peaks at ~1100 and ~800 cm^{-1} typical of SiO_2[27)] are observed in the IR spectrum of the S-F-H powder. The other FSP or ECM-made SiO_2 powders (S-F-S, S-E-H and S-E-S) exhibit mostly the same IR spectra as with S-F-H. A very weak absorption typical of ZnO[27)] is detected in the IR spectrum of Z-F, which resembles that of Z-E. A peak is seen at ~ 900 cm^{-1} for the ZS-F-H and ZS-E-H powders, whereas the ZS-F-S and ZS-E-S powders show two peaks, at ~900 and ~1100 cm^{-1}. Lin and Shen[28)] reported that sol-gel-derived amorphous zinc silicate shows IR absorption at 940 cm^{-1} and argued that the Si-O-Zn linkage shifts the infrared absorption by the Si-O stretching from 1096 cm^{-1} (silica) to 940 cm^{-1}. For ZS-F-H and ZS-E-H, most of the Si-O bonding

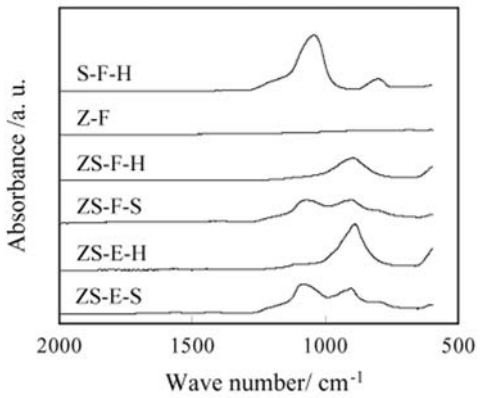

Fig. 6 IR spectra of the product powders. The infrared absorption by the Si-O stretching was shifted from ~1100 cm^{-1} to ~900 cm^{-1} for HMDSO-derived $2ZnO/SiO_2$, suggesting most of the Si-O bonding can be linked (or influenced) with Zn, while the Si-O bonding with and without the influence by Zn co-existed for SiO_2-sol-derived $2ZnO/SiO_2$.

seems linked with (or influenced by) Zn, due to intimate mixing of the Zn with Si species in the gas phase, shifting the IR absorption from ~1100 to ~900 cm^{-1}. These results agree with the XRD results which show that ZnO crystal growth is suppressed by intimate mixing of the Zn with Si species and that zinc silicates are formed partially. For ZS-F-S and ZS-E-S, independent nucleation of ZnO and SiO_2 seems to form the Si-O-Zn linkage partially (e. g. on the surface of the SiO_2 particles), resulting in two absorption peaks at ~ 900 and ~1100 cm^{-1}.

3. 4 Particle formation in the spray flame

Figure 7 shows TEM images of the FSP-made ZnO (Z-F), ECM-made ZnO (Z-E) and FSP-made SiO_2 derived from SiO_2-sol (S-F-S) particles colleted at flame heights of 4, 6 and 8 cm. It was impossible to obtain particles at a flame height of 2 cm because the Cu mesh used for TEM observation melted. For Z-F synthesis (Fig. 7(a)), large particles (e. g. > 100 nm in diameter) are seen on the carbon film at 4 cm, and formation of nanoparticles and their growth are observed at 6 and 8 cm, respectively. These results indicate the Zn species is not evaporated at 4 cm but is completely vaporized by 6 cm. This behavior is substantially different from gas-fed flame aerosol synthesis, where only nanoparticles are seen even at 0.3 cm in flame height.[21] For Z-E synthesis (Fig. 7(b)), submicrometer-sized particles are attached to the Cu mesh at 4 cm although the carbon film is burned out, and large particles still exist on the carbon film at 6 cm, whereas only nanoparticles are observed at 8 cm. The temperature of the emulsion spray flame (ECM), lower than that of the methanol spray flame (FSP), delays the evaporation of the Zn species in the flame, suppressing ZnO particle growth as observed by TEM (Fig. 2) and XRD (Fig. 5). No nanoparticles are observed for S-F-S synthesis (Fig. 7(c)). This observation indicates that evaporation of the Si precursor does not take place in the flame. In addition, the particle size does not change much at 4, 6 and 8 cm although small particles are also seen in the TEMs. This observation suggests that fragmentation of the droplets is completed before 4 cm. Compared with the S-F-S particles collected on the filter (Fig. 2(e)), solid particles rather than hollow ones are seen frequently for S-F-S collected in the flame, although hollow particles also exist (e. g. Fig. 7(c), 6 cm). Sintering may be enhanced for the particles passing through the center of the flame because of a long residence time in the hot zone, favoring solid particle formation.

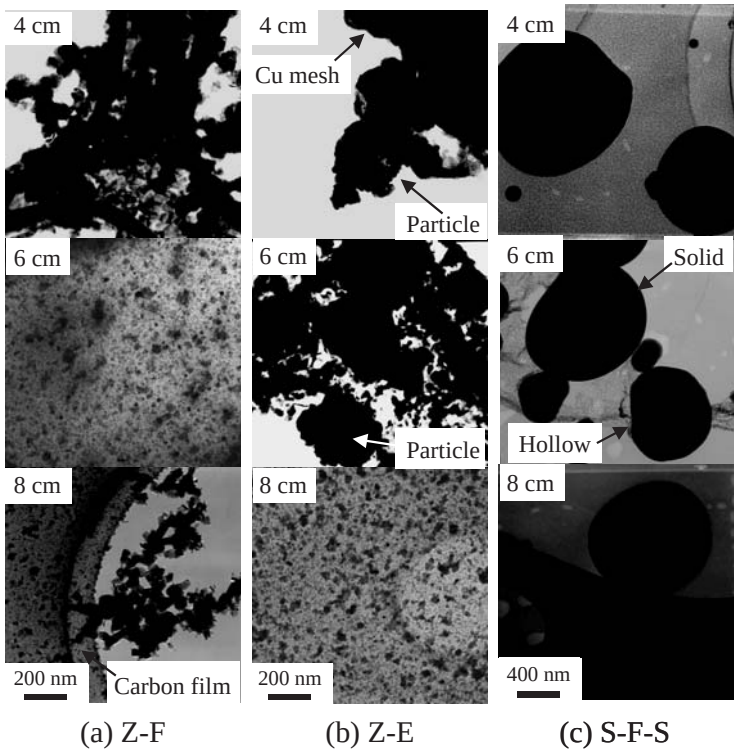

Fig. 7 Morphology of (a) the FSP-made ZnO (Z-F), (b) the ECM-made ZnO (Z-E) and (c) SiO_2-sol-derived SiO_2 by FSP (S-F-S) particles collected at flame heights of 4, 6 and 8 cm by thermophoretic sampling. Complete evaporation of the precursor and particle formation in the gas phase took place at 6 and 8 cm for Z-F and Z-E, respectively, while evaporation of the precursor did not take place for S-F-S.

Figure 8 shows TEM images of the FSP-made 2ZnO/SiO_2 (ZS-F-H and ZS-F-S) particles collected at flame heights of 4, 6 and 8 cm. Submicrometer-sized spherical particles are seen at 4 cm for both ZS-F-H (Fig. 8(a)) and ZS-F-S (Fig. 8(b)) synthesis. These results indicate that the Zn and Si species are not

evaporated at 4 cm as they are for Z-F synthesis (Fig. 7(a)). Only nanoparticles are observed at 6 and 8 cm for S-F-H. This result suggests complete evaporation of the Zn and Si species. A mixture of nanoparticles and large particles (e. g. 100 nm) are formed at 6 cm for ZS-F-S synthesis. This result suggests independent nucleation of ZnO in the gas phase. The large particles (mostly SiO_2) at 6 cm seem smaller in diameter than those at 4 and 8 cm for ZS-F-S, although small particles (e. g. 100-200 nm) are also seen at 4 and 8 cm. These observations suggest that further fragmentation followed by particle growth may take place by evaporation of the Zn species and/or gas generation by decomposition of ZA from the droplets. This mechanism is different from the particle formation of S-F-S (Fig. 7(c)). This results in a smaller diameter for the large particles (mostly SiO_2) in ZS-F-S (Fig. 3(c)) than seen in S-F-S (Fig. 2(e)) and no hollow particle formation of ZS-F-S (Fig. 3(c)). For ZS-F-S and ZS-E-S, the ZnO crystal growth is suppressed compared with the ZnO synthesis (Z-F and Z-E) in spite of independent nucleation of ZnO and SiO_2. Release of the Zn species from the droplets (or fragments) may be delayed because of the presence of SiO_2 for ZS-F-S and ZS-E-S.

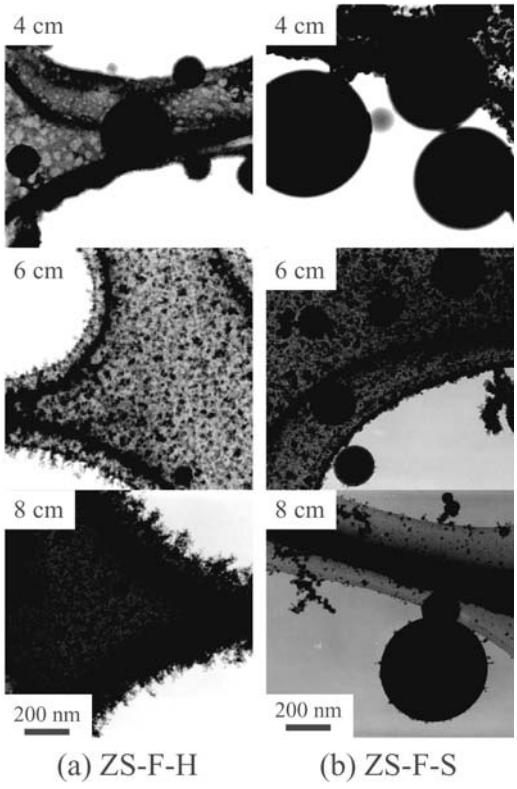

Fig. 8 Morphology of the FSP-made (a) HMDSO-derived $2ZnO/SiO_2$ (ZS-F-H) and (b) SiO_2-sol-derived $2ZnO/SiO_2$ (ZS-F-S) collected at flame heights of 4, 6 and 8 cm by thermophoretic sampling. Both Zn and Si species were evaporated completely at 6 cm for ZS-F-H, whereas ZnO particles were nucleated independently in the gas phase and mixed with SiO_2 particles from the sol for ZS-F-S.

4. Summary

The evolution of particle morphology during FSP synthesis of solid and hollow nanoparticles was investigated by thermophoretic sampling and microscopic analyses. Gas phase reaction takes place for ZnO synthesis from ZA (Z-F and Z-E) and SiO_2 synthesis from HMDSO (S-F-H and S-E-H), forming nanoparticles, whereas submicrometer-sized SiO_2 particles (S-F-S and S-E-S) are created because the SiO_2-sol particles were not evaporated, regardless of the process (FSP or ECM). Thermophoretic sampling showed that complete evaporation of the dispersed droplets takes place along the flame axis for the methanol and emulsion spray flame. The high flame temperature of the methanol spray flame (FSP) probably enhances the release of the metal species to the gas phase, leading to particle growth and resulting in larger d_{BET} and d_{XRD} values for the FSP-made particles as compared with the ECM-made particles prepared from the same precursor for ZnO and SiO_2 synthesis.

Intimate mixing of the Zn and Si species in the gas phase suppresses particle growth, forming nanoparticles with broadened XRD peaks for ZnO and zinc silicates for ZS-F-H and ZS-E-H syntheses, whereas independent nucleation of ZnO and SiO_2 in the gas and liquid phases, respectively, results in a mixture of ZnO nanoparticles and large SiO_2 particles (e. g. 100-300 nm) for ZS-F-S and ZS-E-S syntheses. IR spectra indicated that most Si-O bonding is linked with (or influenced by) Zn for ZS-F-H and ZS-E-H, whereas the Si-O bonding with and without influence of Zn co-exists for ZS-F-S and ZS-E-S, corresponding to intimate mixing and independent nucleation, respectively, of the Zn and Si species. Thermophoretic sampling showed only

nanoparticles for ZS-F-H powder whereas mostly ZnO nanoparticles and large SiO_2 particles co-existed for ZS-F-S powder at 6 and 8 cm in flame height.

The present technique controls the reaction in the flame and thus the particle characteristics can be utilized to optimize dispersion or the level of mixing of two or more oxides for specific mixed oxide systems used in applications such as catalysts (catalyst, promoter and supporting material) and optics (phosphor and stabilizer).

Acknowledgements

This paper was reproduced from J. Am. Ceram. Soc. 87[3] 365-370. Reprinted with permission of the American Ceramic Society, www.ceramics.org. Copyright [March 1, 2004]. All rights reserved.

References

1) Pratsinis, S. E. : Prog. Energy Combust. Sci., **24**-3(1998), 197-219
2) Sokolowski, M., et al. : J. Aerosol. Sci., **8**-4(1977), 219-230
3) Laine, R. M., et al. : Metastable, Mechanically Alloyed and Nanocrystalline Materials, Pts. 1 and 2, **343**-3(2000), 500-510, Trans Tech Publications Ltd, Zurich-Uetikon
4) Limaye, A. U. and Helble, J. J. : J. Am. Ceram. Soc., **85**-5(2002), 1127-1132
5) Mädler, L., et al. : J. Aerosol. Sci., **33**-2(2002), 369-389
6) Kammler, H. K., et al. : Chem. Eng. Technol., **24**-6 (2001), 583-596
7) Mädler, L., et al. : J. Mater. Res., **17**-6(2002), 1356-1362
8) Mikrajuddin, et al. : J. Appl. Phys., **89**-11(2001), 6431-6434
9) Tani, T., et al. : J. Mater. Sci., **37** (2002), 4627-4632
10) Mädler, L., et al. : J. Appl. Phys., **92**-11(2002), 6537-6540
11) Kang, Y. C. and Park, S. B. : Mater. Res. Bull., **35**-7 (2000), 1143-1151
12) Justel, T., et al. : Angew. Chem.-Int. Ed., **37**-22 (1998), 3085-3103
13) Tani, T., et al. : Part. Part. Syst. Charact., **19** (2002), 354-358
14) Lenggoro, I. W., et al. : Jpn. J. Appl. Phys. Pt. 2, Lett., **39**-10B(2000), L1051-L1053
15) Mädler, L. and Pratsinis, S. E. : J. Am. Ceram. Soc., **85**-7(2002), 1713-1718
16) Takatori, K., et al. : J. Nanoparticle Res., **1** (1999), 197-204
17) Tani, T., et al. : J. Mater. Res., **13**-5(1998), 1099-1102
18) Tani, T., et al. : J. Ceram. Soc. Jpn., **109**-12(2001), 981-985
19) Tani, T., et al. : J. Am. Ceram. Soc., **86**-6(2003), 898-904
20) George, A. P., et al. : Symp. Farad. Soc., **1** (1973), 63-71
21) Arabi-Katbi, O. I., et al. : Combust. Flame, **124**-4 (2001), 560-572
22) Tani, T., et al. : J. Am. Ceram. Soc., **87**-3(2004), 365-370
23) Mizutani, Y. : *Nensho-Kogaku* (in Japanese), (1997), Morikita, Tokyo
24) Felder, R. M. and Rouseau, R. W. : Elementary Principles of Chemical Processes, (1986), John Wiley & Sons, New York
25) Klug, H. P. and Alexander, L. E. : X-ray Diffraction Procedures, (1974), John Wiley & Sons, New York
26) Lide, D. R. : CRC Handbook of Chemistry and Physics, 81st ed., (2000), CRC Press, Boca Raton
27) Nyquist, R. A. and Kagel, R. O. : Infrared Spectra of Inorganic Componuds, (1971), Academic Press, Inc., Orlando
28) Lin, C. C. and Shen, P. : J. Non-Cryst. Solids, **171**-3 (1994), 281-289

(Report received on Dec. 13, 2004)

Takao Tani
Research fields : Synthesis of inorganic powders and their applications
Academic degree : Dr. Sc. Techn.
Academic society : Ceram. Soc. Jpn.,

Kazumasa Takatori
Research Field : Inorganic materials
Academic degree : Ph. D.
Academic society : Ceram. Soc. Jpn., Chem. Soc. Jpn.

Sotiris E. Pratsinis*
Research fields : Flame synthesis of functional nanoparticles, Flame-made catalysts, Simulation of Particle Dynamics, Large scale synthesis of nanoparticles
Academic degree : Ph. D.

*Particle Technology Lab., Swiss Fed. Inst.Technol. (ETH), Zurich